

# Optimal Voltage Control in Distribution Systems with Intermittent PV Using Multi-Objective Grey-Wolf-Lévy Optimizer

Karar Mahmoud, Mahmoud M. Hussein, Mohamed Abdel-Nasser, and Matti Lehtonen

**Abstract**— The intermittent photovoltaic (PV) units significantly affect the performance of distribution systems, and they often cause several operational problems, most importantly, voltage rise/drop. At high PV penetration, excessive tap movements of transformers and high curtailed PV power are expected to completely solve the voltage violation problem. In this paper, we propose an optimal voltage control method for distribution systems considering the number of tap movements of transformers and the active power curtailment of PV units. The objective function of the proposed method comprises: 1) voltage drop violation (VDV), 2) voltage rise violation (VRV), 3) tap movement rate (TMR) of transformers, and 4) curtailed power of PV (CPPV). A multi-objective grey wolf optimizer integrated with a Lévy mutation operator (GWO-Lévy) is formulated to accurately solve the voltage control problem. A 24-hour simulation is performed on the 119-bus distribution system with PV and different types of loads. The performance of GWO-Lévy is compared with three other optimizers, finding that it achieves the best performance. The simulation results demonstrate the efficacy of the proposed method for solving the voltage violation problem with PV while simultaneously optimizing TMR and CPPV.

**Index Terms**—Distribution systems; voltage rise; voltage drop; photovoltaic; grey wolf optimizer; Lévy operator.

## I. INTRODUCTION

IT is important to facilitate integrating renewable energy sources (RES), such as solar, wind and hydro, as distributed generations (DG) in distribution systems to reduce greenhouse gas emissions [1]. RES offer a number of advantages besides reducing environmental emissions compared to conventional energy sources, such as lower capital cost, higher security of power supplies, and higher power quality [2]. Consequently, the penetration of RES has been increased rapidly worldwide in the last few decades [3]. However, some RES types, such as photovoltaic (PV), can cause several operational problems in distribution systems because of their intermittent nature [4], [5].

The severity of these operational problems depends on the penetration level of PV systems and their locations in distribution systems [6], [7]. Generally, the distribution systems with high PV penetrations face three categories of challenges: technical, commercial, and regulatory [8]. Voltage violations (i.e., voltage rise/drop) are considered the major technical challenge in distribution systems [9], [10]. The main reason for the voltage violation problem with PV is the reverse power flow at the occasions of low load demand and high PV generation. This reverse power flow may even become bidirectional, which can cause extreme voltage violations, especially at remote feeder ends. To solve the voltage violation problem at these occasions, the PV power could be partially curtailed depending on the regulations of the utility.

In the literature, several methods have been proposed to solve the voltage violation problem in distribution systems with high PV penetration [11], [12]. There are traditional and advanced methods to regulate the voltage within the permissible limits. The traditional methods include on-load tap changer transformers (OLTC), capacitor banks, and step voltage regulators (SVR) in which the control schemes are mechanical in nature. The OLTC at the main substation of the distribution system is considered a vital item to regulate the voltage in the distribution feeders. In turn, SVR is commonly used for regulating the voltage at the downstream feeders. Indeed, most of voltage regulators comprise auto-transformer with on-load tap changers [13]. In long MV distribution feeders, OLTC and SVRs are considered effective devices for voltage regulation. The lifetime of these devices could be dramatically reduced in the case of frequent operations to mitigate rapid voltage variations caused by intermittent PV generation. Based on this feature, it is recommended to minimize the number of operations of these switched-controlled devices. The advanced voltage control methods include active PV power curtailment during low demand and reactive power control of the PV inverter [14], [15]. Another way is to add a leading power factor device which can reduce the amount of PV power curtailment during voltage rise but with extra costs.

The total number of tap movements of OLTC and SVR is a significant factor to be considered when addressing the voltage control problem in distribution systems. Without an efficient coordination between the different voltage control devices, excessive operations of these devices are expected, thereby reducing their lifetime. In [16], a coordinated control method has been proposed for OLTC and switched capacitors to reduce their number of operations. Authors of [17] have presented a coordinated method to prevent the voltage rise problem in low-voltage distribution networks

---

K. Mahmoud is with the Department of Electrical Engineering, Aswan University, 81542 Aswan, Egypt, and also with the Department of Electrical Engineering and Automation, Aalto University, FI-00076 Espoo, Finland (e-mail: karar.alnagar@aswu.edu.eg).

M. Hussein is with the Faculty of Energy Engineering, Aswan University, 81528 Aswan, Egypt (e-mail: mahmoud\_hussein@aswu.edu.eg).

M. Abdel-Nasser is with the Electrical Engineering Department, Aswan University, 81542 Aswan, Egypt, and also with the Department of Computer Engineering and Mathematics, University Rovira i Virgili, 43007 Tarragona, Spain. (e-mail: mohamed.abdelnasser@aswu.edu.eg).

M. Lehtonen is with the Department of Electrical Engineering and Automation, Aalto University, FI-00076 Espoo, Finland (e-mail: matti.lehtonen@aalto.fi).

with PV while relieving the stress on the tap changer. An optimal reactive power control based on forecasting PV power and loads has been formulated in [18] in which the objective function is set to minimize the number of tap movements. Authors of [19] have considered a special configuration of parallel transformers, where losses and tap movements are minimized. In [20], PV systems and parallel OLTCs are managed using different strategies of reactive power control. An interior-point method has been utilized in [21] for voltage control in distribution systems to minimize losses while considering tap movement constraints.

The amount of active PV power curtailment is also a significant issue to be considered for voltage control in distribution systems. In [22], the active power curtailment of PV and the charging/discharging power of electric vehicles are considered as control variables in the voltage control problem. Droop based active power curtailment methods are used in [23] for preventing over-voltage in radial distribution feeders with high PV penetrations. Two different control schemes are applied to a Canadian distribution feeder with twelve consumers and PV. The reduction of PV curtailment is attained in [24] for a practical Chinese power grid with energy storage systems. In [25], curtailment of the output PV power is performed by forcing the interfaced converter of PV not to operate at the maximum power point for the purpose of mitigating voltage fluctuations. In [26], an optimal control method is proposed for minimizing the reactive power of the PV inverter and the curtailed PV power. In [27], a multi-objective approach is proposed to multi-microgrid system design. Three objectives are considered: utility maximization for the microgrids, utility maximization for the power grid, and maximize a sum of the stored energy levels within the multi-microgrid network.

As stated above, OLTC, SVR, and the PV inverter can be used to regulate voltage in distribution systems. The intermittent nature of PV generation and load fluctuations yield excessive tap movements of OLTC and SVR and high amount of the curtailed power of PV. In this paper, an optimal voltage control method for distribution systems with PV is proposed. The objective function of the proposed method includes voltage drop violation (VDV), voltage rise violation (VRV), tap movement rate (TMR) of transformers, and curtailed power of PV (CPPV) terms. A multi-objective grey wolf optimizer (GWO) integrated with a Lévy mutation operator (GWO-Lévy) is employed to minimize the proposed objective function.

Unlike the aforementioned voltage control methods, the proposed method prevents voltage rise and drop problems and optimizes TMR and CPPV, simultaneously. To enable adjusting the priorities of the proposed control method, we incorporate sets of weight factors for each term of the objective function (VDV, VRV, CPPV, and TMR). The weight factors of VRV and VDV are helpful to set buses at which preventing voltage violations has the highest priority. The amount of power curtailment of each PV unit and the rate of tap movements of each transformer can be adjusted using the weight factors of CPPV and TMR, respectively. We incorporate four importance factors for VRV, VDV, TMR, and CPPV in the objective function. These importance factors provide a flexible way to make a trade-off between the different sub-objectives (solving the voltage rise problem, solving the voltage drop problem, reducing TMR of transformers, and reducing the total curtailed PV

power). Furthermore, distribution systems may comprise different areas, and so an importance factor for each area is used to specify the most important area to solve the associated problems with PV.

The rest of this paper is organized as follows. Section II explains the mathematical formulation of the proposed method. The developed grey wolf optimizer with Lévy mutation operator and its implementation to the optimal voltage control are presented in Section III. The results, conclusions and some lines of future work are provided in Sections IV and V, respectively.

## II. PROBLEM FORMULATION

The proposed model for the voltage control problem considers four different sub-objective functions, which quantify VDV, VRV, TMR, and CPPV, to be minimized. The positive feature of this formulation is its ability to set and study the trade-off between the different sub-objectives, and so further control options are available. These sub-objectives are described below.

### A. Voltage drop and rise violations

Considering the real condition of active distribution systems in which upper and lower voltage violations can coexist due to the intermittent PV and load profiles, it is important to model both up-normal conditions. Here, the voltage violation function (VVF) is mathematically expressed as follows:

$$VVF(t_s) = VRV(t_s) + VDV(t_s) \quad (1)$$

in which

$$VRV(t_s) = \sum_{i \in \phi} \left( WF_{VRV,i}(t_s) \times \left( V_i^{max}(t_s) - V_i(t_s) \right)^2 \right) \quad (2)$$

$$VDV(t_s) = \sum_{j \in \phi} \left( WF_{VDV,j}(t_s) \times \left( V_j(t_s) - V_j^{min}(t_s) \right)^2 \right) \quad (3)$$

where  $VRV(t_s)$  and  $VDV(t_s)$  stand for voltage rise violation and voltage drop violation at time  $t_s$ , respectively.  $\phi$  is a list of buses at which the measured/estimated voltages violate the upper voltage limit ( $V^{max}$ ), and  $\phi$  is a list of buses at which the measured/estimated voltages violate the lower voltage limit ( $V^{min}$ ).  $WF_{VRV}$  and  $WF_{VDV}$  represent, respectively, weight factors of  $VRV$  and  $VDV$ , where  $\sum_{i \in \phi} WF_{VRV,i}(t_s) = 1$  and  $\sum_{j \in \phi} WF_{VDV,j}(t_s) = 1$ . These two

sets of weight factors help to set the critical buses at which preventing voltage violations has a higher priority compared to other buses. Note that we have separated the two terms in (1) to allow adjusting an individual weight factor of each term for each bus. The role of the weights in (2) and (3) is to adjust the importance of voltage violations at each bus, not for scaling the objective function.

### B. Tap movement rate (TMR) of transformers

To model tap movements of transformers in the voltage control problem, a formula for TMR is expressed as follows:

$$TMR(t_s) = \sum_{p=1}^N \sum_{k \in \gamma} \left( WF_{TMR,k}(t_s) \times \left( \frac{Tap_k(t_s) - Tap_k(t_{s-p})}{Tap_{k,step}} \right)^2 \right) \quad (4)$$

where  $Tap_k(t_s)$  and  $Tap_k(t_{s-p})$  are the values of the tap of the transformer  $k$  at time  $t_s$  and the previous time  $t_{s-p}$ , respectively;  $\gamma$  is a list of transformers;  $Tap_{k,step}$  is the step

value of the tap of the transformer  $k$ ;  $N$  is the number of the previous time periods to be considered in the current time period  $t_s$ . This formula is based on the fact that the movement of the transformer tap depends on its previous positions and current position.  $WF_{TMR,k}(t_s)$  represents a weight factor for controlling TMR of transformer  $k$  at time  $t_s$  with respect to other transformers, where  $\sum_{k \in \gamma} WF_{TMR,k}(t_s) = 1$ .

The higher value of the weight factor of a transformer, the lower number of tap movements is expected. The role of the weights in (4) is to adjust the tap movement rate of each transformer, not to scale the objective function. Note that the square in equation (4) normalizes the sub-objective function so that its value is only positive.

### C. Curtailed power of PV (CPPV)

The option of curtailing the active PV power is an effective solution for preventing voltage rise by setting the PV converter to curtail a certain amount of the active PV power (i.e., wasting energy). The total CPPV in a distribution system with PV at time  $t_s$  can be formulated as follows:

$$CPPV(t_s) = \sum_{m \in \eta} WF_{CPPV,m}(t_s) \times (PPV_{max,m}(t_s) - PPV_m(t_s))^2 \quad (5)$$

where  $PPV_{max,m}(t_s)$  and  $PPV_m(t_s)$  represent, respectively, the maximum and actual power of the PV unit  $m$  at time  $t_s$ .  $\eta$  is the list of buses connected with PV.  $WF_{CPPV,m}(t_s)$  is a weight factor of the curtailed power of the PV unit  $m$  at time  $t_s$ , where  $\sum_{m \in \eta} WF_{CPPV,m}(t_s) = 1$ . As expressed in (5), we use

weight factors  $(WF_{CPPV,1}, WF_{CPPV,2}, \dots, WF_{CPPV,N_{PV}})$  to adjust the amount of the curtailed power of the individual PV units  $(PV_1, PV_2, \dots, PV_{N_{PV}})$ . For example, if we consider two PV units at buses B1 and B2 where their weighting factors are 1 and 0, respectively. The active power of the first PV unit can be curtailed while the active power of the other unit is not allowed to be curtailed. The use of this sub-objective function ensures a minimum curtailed power of all PV units.

### D. Multi-Objective function

Note that each set of weight factors adjust the weighting of each internal term in the corresponding sub-objective. By adjusting the weight factors, a coordinated control action for OLTC, SVRs, the PV systems can be optimally taken to regulate voltage in distribution systems. Here, other different factors (i.e., importance factors) are introduced to control the importance of each sub-objective with respect to the other objectives. The abovementioned sub-objective functions are formulated as a multi-objective function to be minimized as follows:

$$OF(t_s) = IF_{VRV} \times VRV(t_s) + IF_{VDV} \times VDV(t_s) + IF_{TMR} \times TMR(t_s) + IF_{CPPV} \times CPPV(t_s) \quad (6)$$

where  $IF_{VRV}$ ,  $IF_{VDV}$ ,  $IF_{TMR}$ , and  $IF_{CPPV}$  represent the importance factors of  $VRV$ ,  $VDV$ ,  $TMR$ , and  $CPPV$ , respectively. The main reason of introducing these importance factors is to offer a flexible way to make a trade-off between: 1) solving the voltage rise problem, 2) solving the voltage drop problem, 3) reducing TMR of transformers, and 4) reducing the total curtailed PV power. Note that the sum of the four importance factors is equal to one.

For a distribution system with various areas, where  $\Omega$  is a list of the areas, equation (7) can be formulated as an objective function. As noticed, an importance factor for each area (i.e.,  $IF_{Area,i}$ ) can be set, thereby specifying the most important area to solve the associated problems with PV.

$$TOF = \sum_{i \in \Omega} IF_{Area,i} OF_i(t_s) \quad (7)$$

Note that the four sub-objective functions in the model are transformed into a single objective by utilizing a scaling factor for each sub-objective. In this way, they are normalized to a unified scale. In this paper, we follow [28], [29] in which the maximum of each sub-objective function is used as its scale factor. The values of these scaling factors are high to penalize non-feasible solutions.

### E. Constraints

The following constraints are considered in the proposed voltage control model:

$$CPR_{min,m} \times PPV_{max,m}(t_s) \leq CPPV_m(t_s) \leq CPR_{max,m} \times PPV_{max,m}(t_s), \quad \forall m \in \eta \quad (8)$$

$$-\sqrt{(SPV_m^2 - (PPV_m(t_s) - CPPV(t_s))^2)} \leq RPPV_m(t_s) \leq \sqrt{(SPV_m^2 - (PPV_m(t_s) - CPPV(t_s))^2)}, \quad \forall m \in \eta \quad (9)$$

$$Tap_k^{min} \leq Tap_k(t_s) \leq Tap_k^{max}, \quad \forall k \in \gamma \quad (10)$$

$$(Tap_k(t_{s-1}) - Tap_k(t_s)) / Tap_{k,step} \leq TapR_k, \quad \forall k \in \gamma \quad (11)$$

The constraint (8) represents the upper and lower limits of the curtailed power of each PV unit ( $CPR_{min}$ ,  $CPR_{max}$ ) as a percentage of the maximum PV generation. In this study, the values of  $CPR_{min}$  and  $CPR_{max}$  for all PV units are 0.0 and 1.0, implying that it can curtail the whole PV power. The constraint (9) models the increase in the spare capacity of the PV inverter when the PV power is curtailed, where  $SPV$  is the rated capacity of the PV inverter. Because of power curtailment, additional reactive power of PV inverter ( $RPPV$ ) can be supplied/absorbed, and so contributing positively to regulate voltages. Unlike the other voltage control devices, the reactive power of the PV inverter can rapidly mitigate frequent voltage violations in real time due to intermittent PV generation. This is the reason for providing reactive power independently from the active power injection of PV, and so it is not considered to be minimized. However, the reactive power of PV reduces the lifespan of the inverter and leads to additional losses. Note that the PV inverter may not be effective to significantly reduce the curtailed power during the peak PV generation, unless the PV inverter is oversized to allow further reactive power injection. The constraint (10) models the upper and lower limits of the tap of each transformer. The constraint (11) defines the maximum limit of the number of the tap movements ( $TapR_k$ ) of the transformer  $k$  during the time duration  $(t_s - t_{s-1})$ .

## III. GREY WOLF- LÉVY OPTIMIZER

### A. The grey wolf optimizer (GWO)

The GWO is a swarm-intelligence algorithm which has been applied to several engineering problems [30]. It is inspired from the leadership hierarchy and hunting mechanism of grey wolves. The GWO has assumed the four-level social hierarchy of grey wolves: alpha ( $\alpha$ ) at first,

beta ( $\beta$ ) at second, delta ( $\delta$ ) at third, and finally omega ( $\omega$ ) at last. Alpha wolves are the leaders that manage and conduct the whole pack of wolves. The mathematical model of hunting mechanism of grey wolves includes the following stages: tracking and approaching the prey, encircling the prey until it stops moving, and attacking the prey.

**Encircling Prey:** Grey wolves encircle the prey during the hunt stage which can be formulated as follows:

$$\bar{D} = |\bar{C} \cdot \bar{X}_p(I) - \bar{X}| \quad (12)$$

$$\bar{X}(I+1) = \bar{X}_p(I) - \bar{A} \cdot \bar{D} \quad (13)$$

where  $I$  refers to the current iteration,  $\bar{A}$  and  $\bar{C}$  are coefficient vectors,  $\bar{X}_p(I)$  is the position vector of the prey, and  $\bar{X}$  indicates the position vector of a grey wolf. The vectors  $\bar{A}$  and  $\bar{C}$  can be computed as follows:

$$\bar{A} = 2\bar{a} \cdot \bar{r}_1 - \bar{a}, \quad \bar{C} = 2\bar{r}_2 \quad (14)$$

where  $\bar{a}$  is linearly decreased from 2 to 0 over iterations, and  $r_1$  and  $r_2$  are random vectors in the range [0,1].

**Hunting Stage:** Hunting of a prey is usually guided by  $\alpha$  and  $\beta$  while  $\delta$  wolves participate occasionally. The best candidate solutions ( $\alpha$ ,  $\beta$ , and  $\delta$ ) have a better estimation for the location of the prey, whereas  $\omega$  wolves update their positions according to the position of the three best search agents. The hunt process is formulated as follows:

$$\bar{D}_\alpha = |\bar{C}_1 \cdot \bar{X}_\alpha - \bar{X}|, \bar{D}_\beta = |\bar{C}_2 \cdot \bar{X}_\beta - \bar{X}|, \bar{D}_\delta = |\bar{C}_3 \cdot \bar{X}_\delta - \bar{X}| \quad (15)$$

$$\bar{X}_1 = \bar{X}_\alpha - \bar{A}_1 \cdot (\bar{D}_\alpha), \bar{X}_2 = \bar{X}_\beta - \bar{A}_2 \cdot (\bar{D}_\beta), \bar{X}_3 = \bar{X}_\delta - \bar{A}_3 \cdot (\bar{D}_\delta) \quad (16)$$

$$\bar{X}(I+1) = (\bar{X}_1(I) + \bar{X}_2(I) + \bar{X}_3(I))/3 \quad (17)$$

**Attacking Prey:** To model the process of approaching and hunting the prey, the value of  $\bar{A}$  should be decreased.  $\bar{A}$  is a random value in the interval  $[-2\bar{a}, 2\bar{a}]$ , where  $\bar{a}$  is linearly decreased from 2 to 0 throughout iterations. After the wolves attack the prey, they search for the prey in the next iteration, and they find the next best solution among all wolves. The process is repeated until the termination criterion is reached.

Considering the complexity of objective function and the intermittent nature of PV, the GWO optimizer may be trapped into local minima. To improve the performance of the grey wolf algorithm, Lévy flight is used to produce more efficient results [31]. If GWO cannot find the optimum results in a certain number of iterations, a more efficient search based on Lévy flight is done to prevent trapping to a local optimum. Indeed, the Lévy mutation operator increases the global and local search capabilities. In this paper, a simple method is used to implement the Lévy operator:

$$S = 0.01u(X - X_\alpha) / v^{1/\beta} \quad (18)$$

where  $u$  and  $v$  are random numbers produced by the normal distribution of zero mean and standard deviation of  $\sigma_u^2$  and  $\sigma_v^2$ , respectively.  $S$  is added to the positions of the best wolves computed by (16). It is worth noting that there are abrupt changes in the objective function during the initial steps of iterations, which are decreased gradually over the course of iterations. This behavior can guarantee that the developed optimizer eventually converges.

### B. Implementation of GWO-Lévy to the control model

The proposed optimal voltage control method improves the voltage profile of the distribution system. In this

optimization problem, the control variables are the number of tap movements of transformers, the curtailed power of PV units, and reactive power of the PV inverter. The values of the objective function expressed in (6) are computed with respect to the control variables using the power flow method proposed in [32]. Note that  $\alpha$ ,  $\beta$  and  $\delta$  wolves represent the best three values of the objective function. Fig. 1 shows a flowchart of the proposed voltage control method while the solution steps are listed below:

**Step 1:** Read data of the test system, PV units, and initial tap positions of OLTC and SVR.

**Step 2:** Read the constraints, including upper and lower voltage limits, the upper and lower limits of the curtailed power of each PV unit, the upper and lower limits of the tap of each transformer, and  $TapR$  of each transformer.

**Step 3:** Set the values of search agents and maximum allowed number of iterations. Then, construct the initial population expressed in (19), which considers the constraints, based on the assumed number of wolves.

$$P = \begin{bmatrix} [Tap_1^1 \dots Tap_{N_T}^1] & [CPPV_1^1 \dots CPPV_{N_{PV}}^1] & [RPPV_1^1 \dots RPPV_{N_{PV}}^1] \\ \vdots & \vdots & \vdots \\ [Tap_1^{NS} \dots Tap_{N_T}^{NS}] & [CPPV_1^{NS} \dots CPPV_{N_{PV}}^{NS}] & [RPPV_1^{NS} \dots RPPV_{N_{PV}}^{NS}] \end{bmatrix} \quad (19)$$

**Step 4:** While the current iteration is less than the maximum iteration, perform the following steps:

**Step 4.1:** Run the power flow for each search agent and then calculate the value of the objective function. Then, assign  $\alpha$ ,  $\beta$  and  $\delta$  wolves and the value of the global best solution of the control variables.

**Step 4.2:** Calculate  $D_\alpha$ ,  $D_\beta$ , and  $D_\delta$ :

$$\bar{D}_\alpha = |\bar{C}_1 \cdot \bar{P}_\alpha - \bar{P}|, \bar{D}_\beta = |\bar{C}_2 \cdot \bar{P}_\beta - \bar{P}|, \bar{D}_\delta = |\bar{C}_3 \cdot \bar{P}_\delta - \bar{P}| \quad (20)$$

**Step 4.3:** Apply the Lévy mutation operator as follows:

$$S = 0.01u(P - P_\alpha) / v^{1/\beta} \quad (21)$$

$$\bar{P}_{L1} = \bar{P}_\alpha + S \quad \bar{P}_{L2} = \bar{P}_\beta + S \quad \bar{P}_{L3} = \bar{P}_\delta + S \quad (22)$$

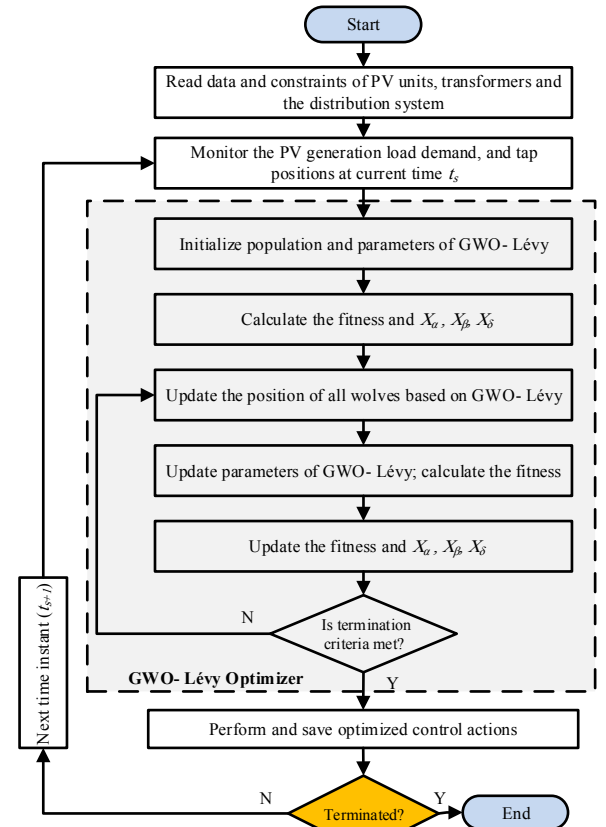


Fig. 1. Flowchart of the proposed voltage control method.

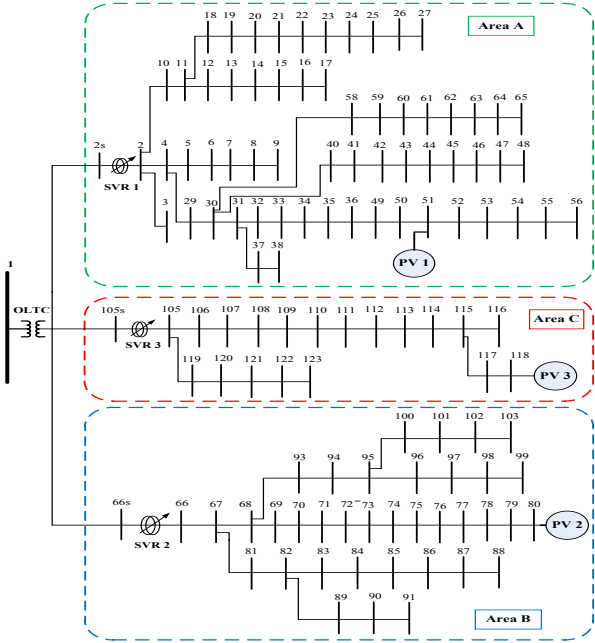


Fig. 2. The modified 119-bus distribution system.

$$\bar{P}_L(I+1) = (\bar{P}_{L1}(I) + \bar{P}_{L2}(I) + \bar{P}_{L3}(I))/3 \quad (23)$$

**Step 5:** If the solution is not converged, go to step 4.1. Otherwise, increment  $t_s$  and go to step 4.

#### Results and Discussions

##### C. Test system

Fig. 2 describes the modified 119-bus distribution system which is used to test the proposed voltage control method. This test system is divided into three areas: 1) Area A includes buses from bus 2 to bus 56, 2) Area B includes buses from bus 66 to bus 103, and 3) Area C includes the buses from bus 105 to bus 123. The modified 119-bus test system in this paper includes three SVR units, OLTC, two PV units, and different load profiles.

The nominal voltage of this system is 11 kV, and the total nominal load demands are 22709.7 kW and 17041.1 kVAR [33]. To demonstrate the effectiveness of the proposed method, real-time simulations are performed for a day with a 5-min time resolution. Different load types (commercial, industrial, domestic and lighting load profiles [34]) are assumed to be distributed in the test system (Fig. 3). It is also assumed that each load profile is treated as a separate load at each bus according to [34]. It is assumed that OLTC is integrated in the main distribution substation, while SVR1, SVR2 and SVR3 are connected to Area A, Area B and Area C, respectively. In this test system, the OLTC unit at the distribution substation is utilized due to its effectiveness in regulating voltage in long distribution feeders. In addition, three PV units (SHARP's NTR5E3E PV 175W module) are connected (PV1, PV2, and PV3 units). PV1 is connected to bus 51 in Area A, PV2 is connected to bus 80 in Area B, and PV3 is connected to bus 118 in Area C. PV1, PV2, and PV3 comprises 300, 1200, 30000 PV modules, respectively. The total PV penetration is 24% with respect to the load demand. Here, a PV unit is located in each area, and the PV locations are selected to be far from the main substation, and they are not optimally determined. Note that the 119-bus test system could not be completely considered as three separate test systems because the OLTC transformer at the distribution substation affects the voltage at all the buses, and the surplus power of a certain area

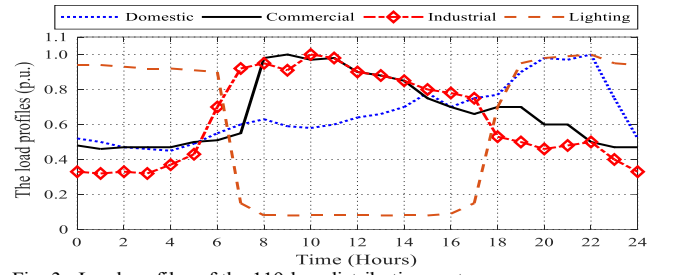


Fig. 3. Load profiles of the 119-bus distribution system.

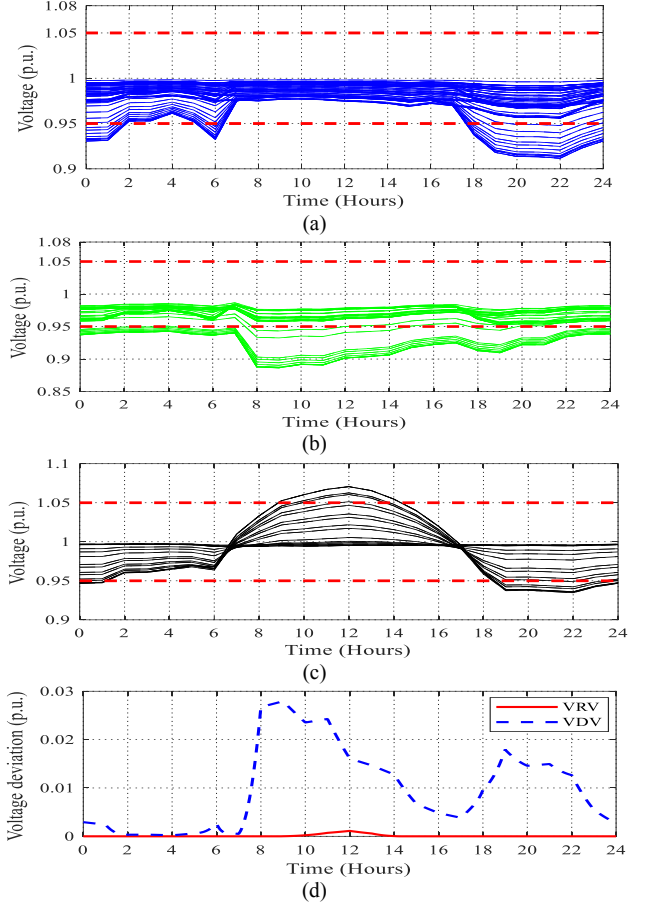


Fig. 4. Voltage profiles of (a) Area A, (b) Area B and (c) Area C; (d) VRV and VDV during the day (Case 0).

(during high PV generation and low demand in this area) can feed the other neighbors' areas. In turn, if the topology of the system is changed, the control system could sense this change, and so it adopts optimal control actions accordingly. It is worth noting that the weight factors of the four sub-objectives are set to be equal in all the simulations except the ones of Subsection E.

##### D. Cases

In our experiments, 24-hour simulations are carried out using the test system. Five cases are studied in this paper:

- **Case 0:** This is the base case in which OLTC, SVR1, SVR2, SVR3, PV1 inverter, PV2 inverter, and PV3 inverter are not employed in the voltage control method.
- **Case 1:** Only *VVF* is considered in the objective function of the proposed method.
- **Case 2:** Both *VVF* and *TMR* are considered in the objective function of the proposed method.
- **Case 3:** Both *VVF* and *CPPV* are considered in the objective function of the proposed method.

TABLE I  
SUMMARY OF THE STUDIED CASES

Cases	Case 0	Case 1	Case 2	Case 3	Case 4
TMR of SVR1	-	139	5	126	2
TMR of SVR2	-	126	3	153	8
TMR of SVR3	-	135	0	144	11
TMR of OLTC	-	127	3	136	5
Total TMR	-	527	11	559	26
CPPV1 (kWh)	-	9.78	9.17	0.07	0.34
CPPV2 (kWh)	-	36.55	39.75	0.3	1.29
CPPV3 (kWh)	-	1006.41	1279.17	21.53	260.60
Total CPPV	-	1052.74	1328.09	21.90	262.23
Total VDV	2.87	0.0	$3.99 \times 10^{-5}$	0.0	$2.15 \times 10^{-5}$
Total VRV	0.03	0.0	$1.97 \times 10^{-5}$	$3.69 \times 10^{-7}$	$2.02 \times 10^{-5}$
Total VVF	2.90	0.0	$5.96 \times 10^{-5}$	$3.69 \times 10^{-7}$	$4.17 \times 10^{-5}$
Total TOF	$15 \times 10^3$	$14 \times 10^3$	$2.6 \times 10^3$	$14 \times 10^3$	$1.9 \times 10^3$

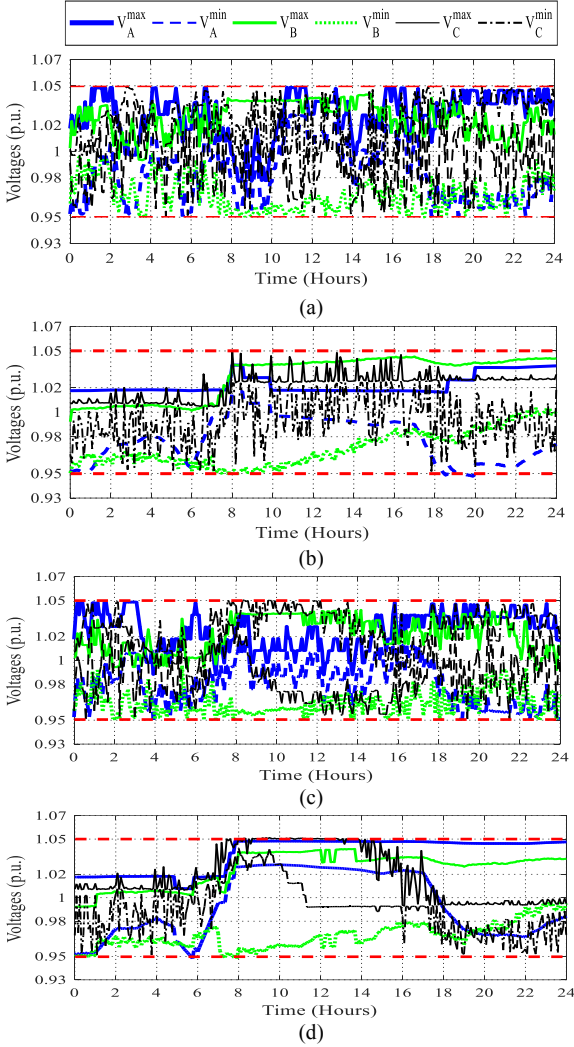


Fig. 5. Voltage profiles of the test system during a day for (a) case 1, (b) case 2, (c) case 3, and (d) case 4.

- **Case 4:**  $VVF$ ,  $TMR$ , and  $CPPV$  are considered in the objective function of the proposed method.

#### E. Analysis of the cases

Fig. 4 shows the voltage profiles of Area A, Area B, and Area C as well as  $VRV$  and  $VDV$  profiles during the day at case 0. As shown, the voltages in Area A and B violate the lower voltage limit (0.95 p.u.) during the night time as indicated in Fig. 4 (a) and Fig. 4 (b), respectively, while the voltages in Area C violate the upper voltage limit (1.05 p.u.) during the daytime as observed in Fig. 4 (c). The profiles of  $VRV$  and  $VDV$  confirm that the test system suffers from voltage rise and the voltage drop at the same time (from

11:00 to 15:00) which make it difficult to solve the voltage violation problem at these occasions.

Table I summaries the results of the proposed voltage control method on the 119-bus distribution system for the five studied cases. It is important to note that case 1, case 2, and case 3 represent the state-of-the-art voltage control methods that consider some sub-objectives and ignore others. In turn, in the proposed method (Case 4), we consider all above-mentioned sub-objectives. As shown in Table I, the voltage violation in case 0 is very high ( $VVF$  equals 2.90). Note that when applying the proposed method in cases 1, 2, 3, and 4, the values of  $VVF$  is decreased to 0.0,  $5.9 \times 10^{-5}$ ,  $3.69 \times 10^{-7}$ , and  $4.17 \times 10^{-5}$ , respectively. This reduction in  $VVF$  implies that the voltage profiles are significantly improved by using the proposed method for the four cases. Fig. 5 (a, b, c, and d) illustrates this improvement where the voltage profiles of the system are shown during the day for case 1, case 2, case 3, and case 4, respectively. In Fig. 5, we have plotted only the minimum and maximum voltage for each area. Note that  $V_X^{\max}$  and  $V_X^{\min}$  refer to the maximum and the minimum voltages of Area X, respectively. It is noticed that in all cases (except case 0), the voltage profiles are maintained within the specified limits. In general, we can observe that the voltage profiles in case 1 are considered the best case (total  $VVF=0.0$ ) because the  $VVF$  sub-function is only optimized.

In case 2, the proposed control method minimizes  $VVF$  and  $TMR$ . As a result, the total number of tap movements during the day, in this case, is significantly lower than  $TMR$  values in the other cases. The total  $TMR$  is 11 in this case, and it is 527, 559, and 26 for case 1, case 3, and case 4, respectively. The number of tap movements in cases 1 and 3 is high and not realistic. To ensure minimum and realistic tap movements during the day, we should consider the  $TMR$  sub-objective (accomplished in cases 2 and 4). Regarding case 3, the proposed control method minimizes  $VVF$  and  $CPPV$ . As a result, the value of  $CPPV$  is significantly lower than  $CPPV$  values of the other cases. For instance, the total  $CPPV$  value is 21.9 kWh in this case, and it is 1052.74 kWh, 1328.09 kWh, and 260.60 kWh for case 1, case 2, and case 4, respectively. When considering the sub-objective of the PV curtailed power (i.e., case 3 and 4), the curtailed power of PV3 is higher than PV1 and PV2 (Table I). This is because PV3 causes high voltage rise in the base case (Fig. 4.c) compared to PV1 and PV2. For example, in case 4, the curtailed power of PV3 is 260.6 kWh while only 0.34 kWh and 1.29 kWh are curtailed from PV1 and PV2, respectively.

Indeed, cases 1, 2, and 3 have a superior feature in terms of  $VVF$ ,  $TMR$ , and  $CPPV$ , respectively. In other words, none of these cases consider the different aspects of distribution systems with PV. In turn, in case 4, the proposed control method optimizes the values of  $VVF$ ,  $TMR$ , and  $CPPV$ . Therefore, the proposed control method, in this case, is considered a comprehensive control method because it optimizes all sub-objective functions simultaneously.

Fig. 6 shows the variation of the sub-objective functions during the day, including the normalized PV curtailed power, cumulative tap movements, and normalized PV reactive power of the proposed method for case 1 (Fig. 6 a,b,c), case 2 (Fig. 6 d,e,f), case 3 (Fig. 6 g,h,i), and case 4 (Fig. 6 j,k,l). It is noticed that the amount of the total curtailed PV power values in case 3 and case 4 are lower than case 1 and case 2. The reason for this trend is that the

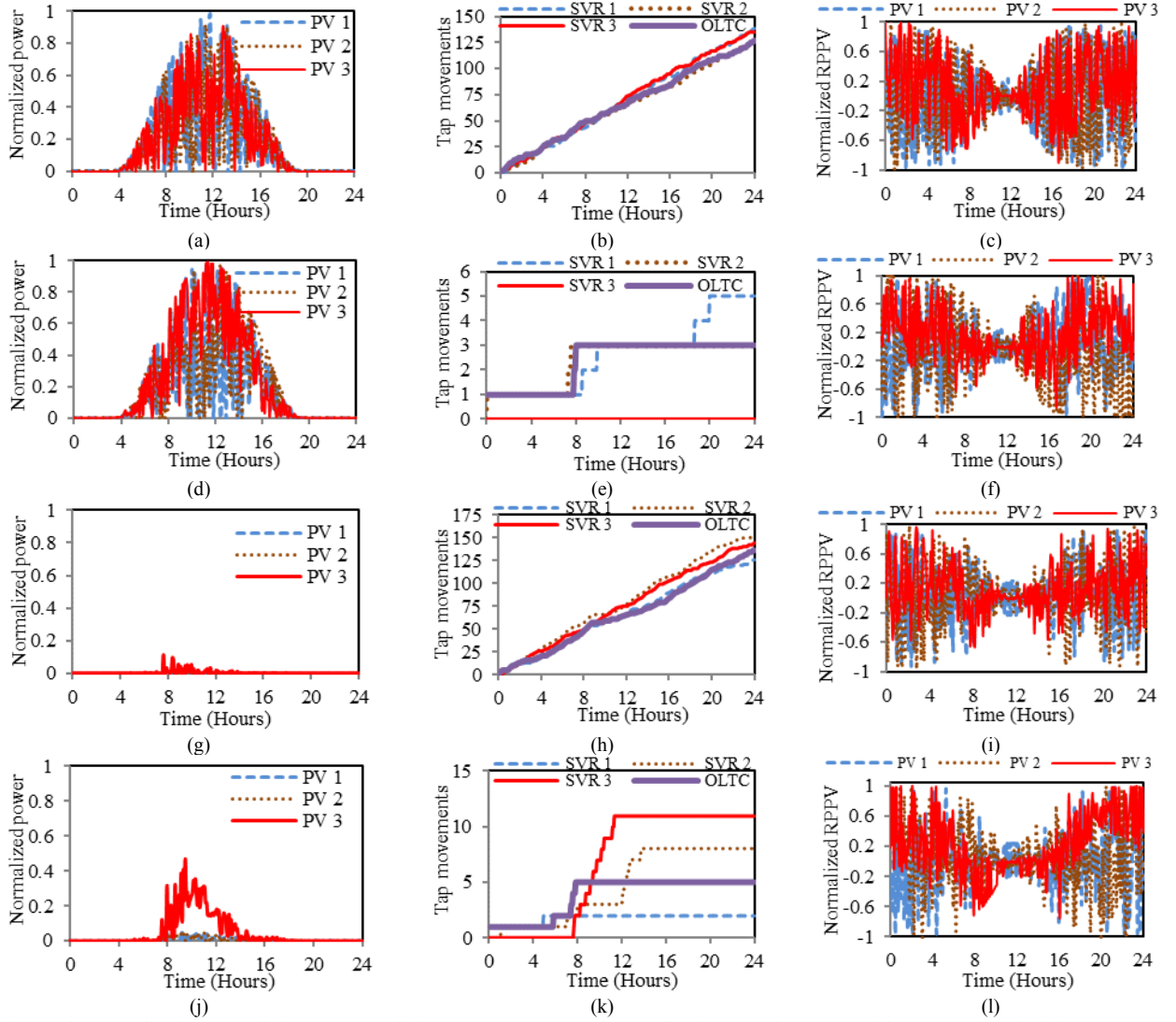


Fig. 6. The normalized PV curtailed power, cumulative tap movements, and normalized PV reactive power of the proposed method for case 1 (a,b,c), case 2 (d,e,f), case 3(g,h,i), and case 4 (j,k,l).

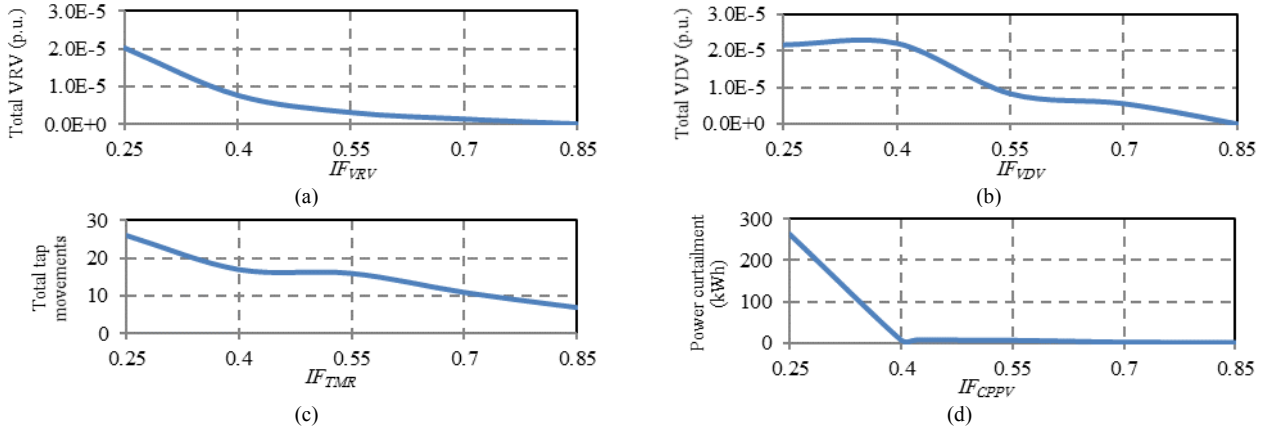


Fig. 7. The effect of increasing the importance factors on the sub-objective functions.

CPPV is only considered in case 3 and case 4. On the contrary, in case 2 and case 4 which consider TMR, the total numbers of tap movements are relatively small compared with cases 1 and 3.

The variations of normalized reactive power injections of PV units, which are constrained with the spare capacity of the inverter, are shown in Fig. 6 (c,f,i,l) during the day for the cases. It is worth to note that reactive power injections during the night time are higher than the daytime. The reason behind this behavior is that the spare capacity of PV is small at the daytime due to high PV active generation

while it is high (full capacity of the PV inverter) during the night. It is important to note that the grey wolf optimizer with Lévy mutation operator consumes in terms of seconds per each time step. This execution time is much lower than the time resolution of the control method (5 min).

#### F. Effect of the importance factors of the sub-objectives

Fig. 7 shows the variation of  $VRV$ ,  $VDV$ ,  $TMR$ , and  $CPPV$  with changing  $IF_{VRV}$ ,  $IF_{VDV}$ ,  $IF_{TMR}$ , and  $IF_{CPPV}$ , respectively. In this experiment, the importance factor of each objective function is increased from 0.25 to 0.85 with a step of 0.15

while the other three importance factors are kept equal and decreased with a step of 0.05. Fig. 7 (a) shows the effect of increasing  $IF_{VRV}$  from 0.25 to 0.85 on VRV. It is observed that VRV decreases from  $2.02 \times 10^{-5}$  to 0.0. Similar to  $VRV$ ,  $VDV$  also decreases from  $2.15 \times 10^{-5}$  to 0.0 with increasing its weight factor from 0.25 to 0.85, as shown in Fig. 7 (b). These results demonstrate the flexibility of the proposed method to focus on enhancing  $VRV$  and/or  $VDV$  in distribution systems by a proper setting of the corresponding importance factors.

Fig. 7 (c) shows the effect of increasing  $IF_{TMR}$  from 0.25 to 0.85 on the total number of tap movements (i.e.,  $TMR$ ) of OLTC, SVR1, SVR2, and SVR3 during the day. It is interesting to note that the total number of tap movements decreases from 26 to 7 when increasing  $IF_{TMR}$  from 0.25 to 0.85. This trend implies that the higher value of  $IF_{TMR}$  in the objective function, the lower number of tap movements is attained. The total curtailed power of PVs decreases from 226 kWh to 1.66 kWh with increasing its importance factor from 0.25 to 0.85, as shown in Fig. 7 (d). This reduction in total curtailed PV power saves energy of PVs.

Indeed, the effect of increasing the importance factors on the sub-objective functions could be different if other PV installations and distribution systems are considered, but similar trends are expected in other systems (decreasing each sub-objective with increasing its importance factor). The solution of a multiple objective optimization is a set of non-dominated solutions (Pareto-front). The Pareto front is important because it can demonstrate how one objective affects the others. This simulation can be a helpful tool for the distribution system operators to allow further control options with conflicting objectives. The proposed method is able to achieve Pareto-front optimal solutions, providing distribution system operators further control options.

### G. Effect of the weight factors

In this subsection, we study the variation of the total TMR of OLTC for the day with increasing its weight factor ( $WF_{TMR,OLTC}$ ). In this analysis,  $WF_{TMR,OLTC}$  is increased from 0.4 to 0.85 with a step of 0.15 while the weight factors of SVR1, SVR2, and SVR3 are kept equal and decreased with a step of 0.05. As shown in Fig. 8, the number of tap movements decreases from 5 to 1, and the percentage of TMR of OLTC with respect to the total TMR of transformers decreases from 13.5 to 1.8, when increasing  $WF_{TMR,OLTC}$  from 0.4 to 0.85. The number of tap movements of OLTC is decreased at the expense of SVR1, SVR2, and SVR3. This analysis highlights the importance of the proposed method to the system operators for adjusting the duty of each transformer for solving the voltage control problem.

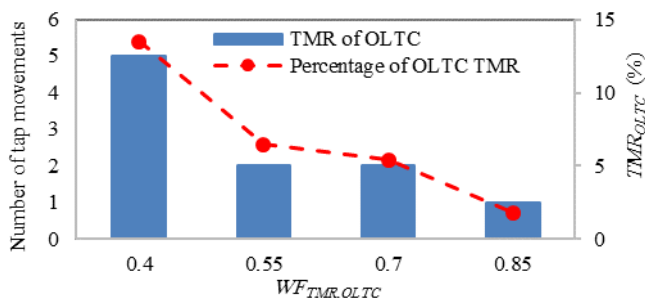


Fig. 8. The variation of the total TMR of OLTC for the day with increasing its weight factor.

### H. High PV scenarios

Table II describes the performance of the proposed control method with high PV penetrations. In this analysis, the test system is simulated with three scenarios of PV penetrations (scenario 1, scenario 2, and scenario 3). Scenarios 1, 2, and 3 comprise 125, 150, and 200 % of the base PV size, respectively. The VVF values are  $14.06 \times 10^{-5}$ ,  $10.01 \times 10^{-5}$ , and  $13.06 \times 10^{-5}$  for scenarios 1, 2 and 3, respectively. The total tap movements and total PV power curtailment increase with rising the PV penetration whereas the voltages are still within the permissible limits. The results demonstrate the high performance of the proposed control method for regulating voltage in the case of high PV penetrations.

TABLE II  
THE PERFORMANCE OF THE PROPOSED METHOD UNDER DIFFERENT SCENARIOS OF PV PENETRATION

PV Scenarios	Scenario 1	Scenario 2	Scenario 3
TMR of SVR1	20	21	32
TMR of SVR2	7	5	8
TMR of SVR3	18	20	24
TMR of OLTC	16	19	26
Total TMR	61	65	90
CPPV1 (kWh)	0.43	0.59	0.74
CPPV2 (kWh)	1.65	2.53	3.33
CPPV3 (kWh)	173.55	248.48	264.83
Total CPPV	175.63	251.6	268.90
Total VDV	$13.21 \times 10^{-5}$	$7.90 \times 10^{-5}$	$10.34 \times 10^{-5}$
Total VRV	$0.85 \times 10^{-5}$	$2.11 \times 10^{-5}$	$2.72 \times 10^{-5}$
Total VVF	$14.06 \times 10^{-5}$	$10.01 \times 10^{-5}$	$13.06 \times 10^{-5}$

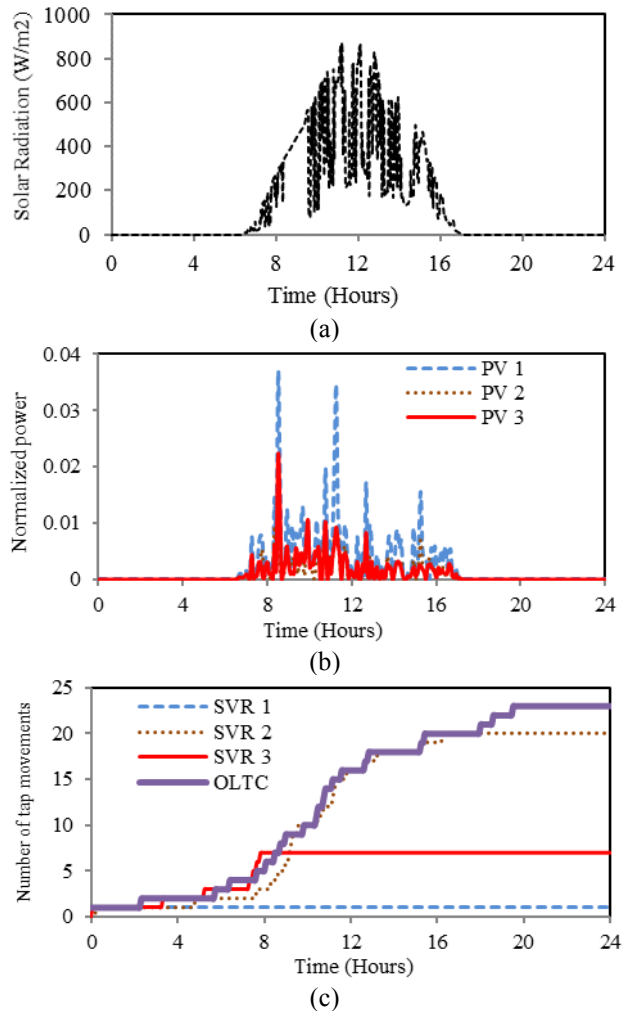


Fig. 9. Results of a fluctuated PV generation profile. (a) solar radiation, (b) curtailed power of PV units, and (c) cumulative tap movements.

### I. Fluctuated PV profile

Here, the proposed voltage control method is tested considering a fluctuated PV profile. Fig. 9 (a) shows the solar radiation during the studied day where high fluctuations are noticed. The curtailed PV power during the day is shown in Fig. 9 (b). It is clear that the amount of the curtailed power is small during the fluctuated day (less than 4 % of the PV nominal power) compared with that of the clear day shown in Fig. 6(j). Regarding the tap movement shown in Fig. 9(c), high tap movement rates of the transformers are also noticed compared with the clear day.

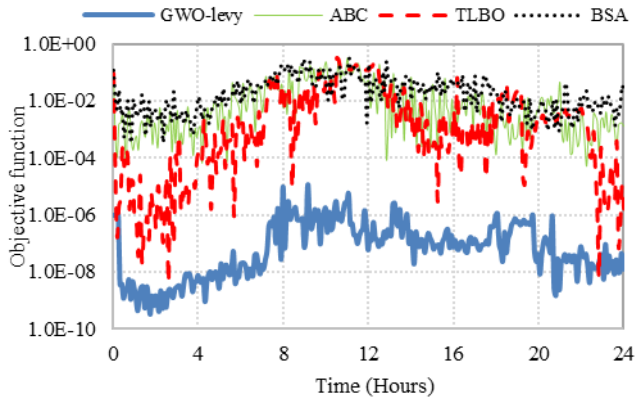


Fig. 10. Performance evaluation of the different optimizers.

### J. Performance Evaluation of GWO-Lévy

In this subsection, the performance of the utilized GWO-Lévy optimizer is compared with three other optimizers: 1) artificial bee colony (ABC) algorithm [35], 2) teaching-learning-based optimization (TLBO) algorithm [36], and 3) backtracking search optimization algorithm (BSA) [37]. Fig. 10 shows the values of the objective function during a day. It is noticeable that the GWO-Lévy has the best performance since it yields the lowest values of the objective function during the day compared with the other optimizers.

In the simulations, the GWO-Lévy takes a few seconds per each time step of the proposed control method. This execution time is much lower than the time resolution of the proposed control method (5 min). We suggest the following possible two approaches for the case that such execution time is required to be reduced. The first approach is to develop a parallel version of the GWO-Lévy while utilizing high-performance computing for reducing the computational burden. The second approach is to exploit short-term forecasting models for PV and load demand [38]. For instance, let the current time instant  $t_s$ , the optimization model at the next time instant  $t_{s+1}$  can be solved in advance based on the predicted PV power and load demand. Note that such approaches are not investigated here and are left for future study.

## IV. CONCLUSIONS

Several operational problems are associated with high PV penetrations in distribution systems, including voltage rise/drop, excessive tap movements of OLTC and SVRs, and high curtailed power of PV systems. In this paper, we have proposed an optimal voltage control method to completely solve the voltage violation problem in distribution systems while optimizing the number of tap movements of transformers and the active power

curtailment of PV units. The proposed objective function involves: VDV, VRV, TMR, and CPPV sub-objectives, considering the different constraints of the distribution systems, transformers, and PV. The multi-objective grey wolf optimizer with a Lévy mutation operator has been used to efficiently solve the nonlinear voltage control model. We have carried out 24-hour simulations on the large-scale 119-bus distribution system with three PV units and different types of loads. The simulation results show that the proposed method can properly solve the voltage violation problem with PV. The positive feature of the proposed method is that it optimizes TMR (increase lifetime of transformers) and CPPV (save energy), simultaneously. The future work will be directed to consider different types of RES and load response in the voltage control problem. In addition, the uncertainties of load and PV generations will be considered.

## REFERENCES

- [1] M. Hosenuzzaman, N. A. Rahim, J. Selvaraj, M. Hasanuzzaman, A. B. M. A. Malek, and A. Nahar, "Global prospects, progress, policies, and environmental impact of solar photovoltaic power generation," *Renew. Sustain. Energy Rev.*, vol. 41, pp. 284–297, 2015.
- [2] F. Shariatzadeh, P. Mandal, and A. K. Srivastava, "Demand response for sustainable energy systems: A review, application and implementation strategy," *Renew. Sustain. Energy Rev.*, vol. 45, pp. 343–350, 2015.
- [3] K. M. Muttaqi, A. D. T. Le, M. Negnevitsky, and G. Ledwich, "A coordinated voltage control approach for coordination of OLTC, voltage regulator and DG to regulate voltage in a distribution feeder," in *2013 IEEE Industry Applications Society Annual Meeting*, 2013, pp. 1–8.
- [4] J. Jung, A. Onen, R. Arghandeh, and R. P. Broadwater, "Coordinated control of automated devices and photovoltaic generators for voltage rise mitigation in power distribution circuits," *Renew. Energy*, vol. 66, pp. 532–540, 2014.
- [5] S. Vazquez, S. M. Lukic, E. Galvan, L. G. Franquelo, and J. M. Carrasco, "Energy Storage Systems for Transport and Grid Applications," *IEEE Trans. Ind. Electron.*, vol. 57, no. 12, pp. 3881–3895, 2010.
- [6] K. Mahmoud, N. Yorino, and A. Ahmed, "Optimal Distributed Generation Allocation in Distribution Systems for Loss Minimization," *IEEE Trans. Power Syst.*, vol. 31, no. 2, pp. 960–969, 2016.
- [7] Q. Li, R. Ayyanar, and V. Vittal, "Convex Optimization for DES Planning and Operation in Radial Distribution Systems With High Penetration of Photovoltaic Resources," *IEEE Trans. Sustain. Energy*, vol. 7, no. 3, pp. 985–995, Jul. 2016.
- [8] M. Karimi, H. Mokhlis, K. Naidu, S. Uddin, and A. H. A. Bakar, "Photovoltaic penetration issues and impacts in distribution network - A review," *Renew. Sustain. Energy Rev.*, vol. 53, pp. 594–605, 2016.
- [9] B. Bletterie, S. Kadam, R. Bolgarny, and A. Zegers, "Voltage Control with PV Inverters in Low Voltage Networks—In Depth Analysis of Different Concepts and Parameterization Criteria," *IEEE Trans. Power Syst.*, vol. 32, no. 1, pp. 177–185, Jan. 2017.
- [10] A. Y. Elrayah, M. Z. C. Wanik, and A. Bouselham, "Simplified Approach to Analyze Voltage Rise in LV Systems With PV Installations Using Equivalent Power Systems Diagrams," *IEEE Trans. Power Deliv.*, vol. 32, no. 4, pp. 2140–2149, Aug. 2017.
- [11] K. W. Kow, Y. W. Wong, R. K. Rajkumar, and R. K. Rajkumar, "A review on performance of artificial intelligence and conventional method in mitigating PV grid-tied related power quality events," *Renew. Sustain. Energy Rev.*, vol. 56, pp. 334–346, Apr. 2016.
- [12] T. Dragicevic, X. Lu, J. C. Vasquez, and J. M. Guerrero, "DC Microgrids - Part I: A Review of Control Strategies and Stabilization Techniques," *IEEE Trans. Power Electron.*, vol. 31, no. 7, pp. 4876–4891, 2016.
- [13] D. Ranamuka, A. P. Agalgaonkar, and K. M. Muttaqi, "Online Voltage Control in Distribution Systems With Multiple Voltage Regulating Devices," *IEEE Trans. Sustain. Energy*, vol. 5, no. 2, pp. 617–628, Apr. 2014.
- [14] S. N. Liew and G. Strbac, "Maximising penetration of wind

- generation in existing distribution networks," *IEE Proc. - Gener. Transm. Distrib.*, vol. 149, no. 3, p. 256, May 2002.
- [15] N. Mahmud and A. Zahedi, "Review of control strategies for voltage regulation of the smart distribution network with high penetration of renewable distributed generation," *Renew. Sustain. Energy Rev.*, vol. 64, no. December, pp. 582–595, 2016.
- [16] J. Y. Park, S. R. Nam, and J. K. Park, "Control of a ULTC considering the dispatch schedule of capacitors in a distribution system," *IEEE Trans. Power Syst.*, vol. 22, no. 2, pp. 755–761, 2007.
- [17] X. Liu, A. Aichhorn, and L. Liu, "Coordinated Control of Distributed Energy Storage System With Tap Changer Transformers for Voltage Rise Mitigation Under High Photovoltaic Penetration," *IEEE Trans. Smart Grid*, vol. 3, no. 2, pp. 897–906, 2012.
- [18] R. M. Mohan, P. B. Prasad, and O. L. N. Kesavulu, "Voltage Control in Distribution Network Considering the Impact of PV Generation on Tap Changers and Autonomous Regulators," *Int. J. Electr. Eng.*, vol. 10, no. 2, pp. 143–156, 2017.
- [19] L. Chen and H. Li, "Optimized Reactive Power Supports Using Transformer Tap Stagger in Distribution Networks," *IEEE Trans. Smart Grid*, vol. 8, no. 4, pp. 1987–1996, 2017.
- [20] M. Krafczy, T. Stetz, and M. Braun, "Parallel Operation of Transformers with On-load Tap Changer and Photovoltaic Systems with Reactive Power Control," *IEEE Trans. Smart Grid*, vol. 3053, no. c, pp. 1–1, 2017.
- [21] M. B. Liu, C. A. Cañizares, and W. Huang, "Reactive Power and Voltage Control in Distribution Systems with Limited Switching Operations," *IEEE Trans. Power Syst.*, vol. 24, no. 2, pp. 889–899, 2008.
- [22] M. Zeraati, M. E. H. Golshan, and J. M. Guerrero, "A Consensus-Based Cooperative Control of PEV Battery and PV Active Power Curtailment for Voltage Regulation in Distribution Networks," *IEEE Trans. Smart Grid*, vol. 3053, no. c, pp. 1–1, 2017.
- [23] R. Tonkoski, L. A. C. Lopes, and T. H. M. El-Fouly, "Coordinated active power curtailment of grid connected PV inverters for overvoltage prevention," *IEEE Trans. Sustain. Energy*, vol. 2, no. 2, pp. 139–147, 2011.
- [24] S. Ma, Y. P. Xu, X. F. Li, Y. F. Wang, N. Zhang, and Y. R. Xu, "Research on Reduction of Solar Power Curtailment with Grid Connected Energy Storage System Based on Time-Series Production Simulation," *Energy Power Eng.*, vol. 9, pp. 162–175, 2017.
- [25] W. A. Omran, M. Kazerani, and M. M. A. Salama, "Investigation of methods for reduction of power fluctuations generated from large grid-connected photovoltaic systems," *IEEE Trans. Energy Convers.*, vol. 26, no. 1, pp. 318–327, 2011.
- [26] B. Zhao, Z. Xu, C. Xu, C. Wang, and F. Lin, "Network Partition Based Zonal Voltage Control for Distribution Networks with Distributed PV Systems," *IEEE Trans. Smart Grid*, vol. PP, no. 99, pp. 1–1, 2017.
- [27] W.-Y. Chiu, H. Sun, and H. Vincent Poor, "A Multiobjective Approach to Multimicrogrid System Design," *IEEE Trans. Smart Grid*, vol. 6, no. 5, pp. 2263–2272, Sep. 2015.
- [28] X. Su, M. A. S. Masoum, and P. J. Wolfs, "PSO and Improved BSFS Based Sequential Comprehensive Placement and Real-Time Multi-Objective Control of Delta-Connected Switched Capacitors in Unbalanced Radial MV Distribution Networks," *IEEE Trans. Power Syst.*, vol. 31, no. 1, pp. 612–622, Jan. 2016.
- [29] R. T. Marler and J. S. Arora, "The weighted sum method for multi-objective optimization: new insights," *Struct. Multidiscip. Optim.*, vol. 41, no. 6, pp. 853–862, Jun. 2010.
- [30] S. Mirjalili, S. M. Mirjalili, and A. Lewis, "Grey wolf optimizer," *Adv. Eng. Softw.*, vol. 69, pp. 46–61, 2014.
- [31] S. Amirsadri, S. J. Mousavirad, and H. Ebrahimpour-Komleh, "A Levy flight-based grey wolf optimizer combined with back-propagation algorithm for neural network training," *Neural Comput. Appl.*, pp. 1–14, May 2017.
- [32] N. Yorino and K. Mahmoud, "Robust quadratic-based BFS power flow method for multi-phase distribution systems," *IET Gener. Transm. Distrib.*, vol. 10, no. 9, pp. 2240–2250, Jun. 2016.
- [33] D. Zhang, Z. Fu, and L. Zhang, "An improved TS algorithm for loss-minimum reconfiguration in large-scale distribution systems," *Electr. Power Syst. Res.*, vol. 77, no. 5–6, pp. 685–694, Apr. 2007.
- [34] R. Taleski and D. Rajcic, "Energy summation method for energy loss computation in radial distribution networks," *IEEE Trans. Power Syst.*, vol. 11, no. 2, pp. 1104–1111, May 1996.
- [35] D. Karaboga and B. Basturk, "A powerful and efficient algorithm for numerical function optimization: artificial bee colony (ABC) algorithm," *J. Glob. Optim.*, vol. 39, no. 3, pp. 459–471, Oct. 2007.
- [36] R. V. Rao, V. J. Savsani, and D. P. Vakharia, "Teaching-learning-based optimization: A novel method for constrained mechanical design optimization problems," *Comput. Des.*, vol. 43, no. 3, pp. 303–315, Mar. 2011.
- [37] P. Civicioglu, "Backtracking Search Optimization Algorithm for numerical optimization problems," *Appl. Math. Comput.*, vol. 219, no. 15, pp. 8121–8144, Apr. 2013.
- [38] M. Abdel-Nasser and K. Mahmoud, "Accurate photovoltaic power forecasting models using deep LSTM-RNN," *Neural Comput. Appl.*, Oct. 2017.